Scalable Flat-Panel Nano-Particle MEMS/NEMS Thruster

IEPC-2005-176
Presented at the 29th International Electric Propulsion Conference, Princeton University
October 31 – November 4, 2005

L. Musinski*, T. Liu†, B. Gilchrist‡, A. Gallimore§, M. Keidar**
University of Michigan, Ann Arbor, MI 48109, USA

Abstract

A new electrostatic thruster technology appears feasible using nano-particles with micro- and nano-electromechanical systems (NEMS/MEMS) fabrication technology. MEMS technologies are already being explored as a possible approach to achieve scalability and system simplification by creating higher efficiency "flat panel" thrusters. They also appear to offer a way to eliminate life-limiting physical characteristics present in state-of-the-art ion propulsion by eliminating the need for a discharge chamber and reducing or eliminating charge-exchange (CEX) collision effects in the ion optics region of the thruster. Further, by considering the use of nano-particles as a propellant with *electric field-emission* based MEMS/NEMS thruster concepts, important new performance improvements appear possible. These include (1) operations at high power levels at much lower system-level specific mass, (2) even higher efficiency, (3) a further increase in thrust densities over present-day ion propulsion technologies, and (4) the ability to tune desired thrust characteristics by simply changing nano-particle size and shape. At the University of Michigan, the nano-particle electrostatic propulsion concept is called nanoFET (nano-Field Emission Thruster) and can be thought of as a flat-panel ion thruster that can be designed for variable power and particle sizes.

Nomenclature

A	=	Thruster area	P	=	Power
C_d	=	Coefficient of drag	q	=	Charge
d	=	Diameter of particle	r	=	Particle radius
E_l	=	Applied electric field in liquid	ρ	=	Mass density of particle
ε_l	=	Liquid dielectric constant	ρ_l	=	Mass density of liquid
ε_o	=	Free space dielectric const	n	=	# density of particles
F_c	=	Coulomb force	T	=	Thrust
F_d	=	Drag force	τ	=	Relaxation time constant
g	=	Earth's gravitational constant	v	=	Particle velocity
γ	=	Surface tension	V_o	=	Voltage
I_{sp}	=	Specific impulse			
l	=	Particle length			
m	=	Particle mass			

* Graduate Student, Electrical Engineering, louisdm@umich.edu
† Graduate Student, Aerospace Engineering, liutm@umich.edu
‡ Professor, Electrical Engineering and Space Science, gilchrst@umich.edu
§ Professor, Aerospace Engineering, rasta@umich.edu
** Professor, Aerospace Engineering, keidar@umich.edu

I. Concept Overview

Figure 1 is a simplified systems sketch of the flat-panel MEMS/NEMS based thruster concept that uses both nano-particles and ions as propellant. Figure 2 shows a present-day ion thruster block-diagram for comparison. The ion thruster must create plasma using a gas (e.g. Xe) in a chamber and allow the ions to escape across an accelerating grid structure. There are several practical limitations: (1) the ionization process represents an important life-limiting factor, (2) an important fraction of the propellant is never ionized, and (3) the plasma interacts with the walls and the grid, thus generating waste heat and limiting lifetime[5].

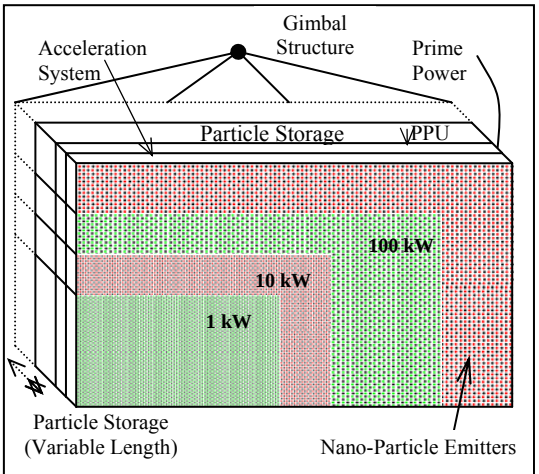

Figure 1: Concept sketch of a flat-panel nano-particle and ion MEMS/NEMS thruster.

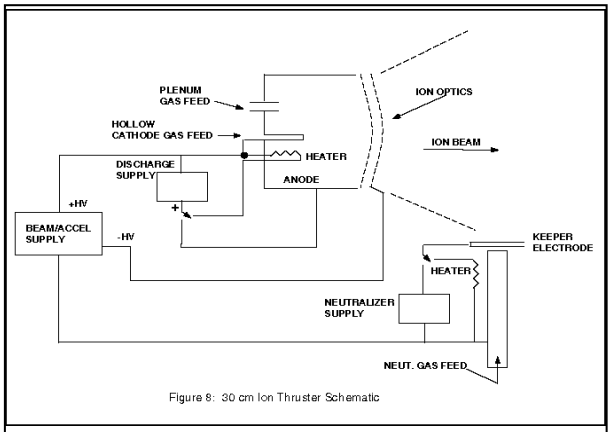

Figure 2: Block diagram of a present-day ion thruster system[13].

In contrast, at the core of the flat-panel thruster, we propose to use millions of MEMS/NEMS based micron-size vias, similar to what is shown in Figure 3, that have a multi-layer grid to establish critical electric-field levels to extract and accelerate either ions using field emission from a conducting liquid (e.g. indium) or, in a different section of the thruster, charged conducting nano-particles (Figure 4) from the surface of either an insulating or mildly conducting liquid used to transport the particles. These nano-particles will range in size from below 0.1 nm to over 100 nm.

The concept of utilizing field emission and electrostatic acceleration of ions is well known as Field Emission Electric Propulsion (FEEP). FEEP thrusters can produce specific impulses above 10,000 seconds at electrical efficiencies exceeding 90% using melted metal liquid propellant such as indium[3,13]. However, FEEPs use needle-like emitters that require footprints many of times wider than the needle tips. Thus, their potential for being scaled-up to say multi-kW power levels is doubtful. Our concept proposes to use highly scalable MEMS/NEMS technologies applied to both nano-particle and ion propulsion and is referred to as nano-Field Emission Thruster (nanoFET).

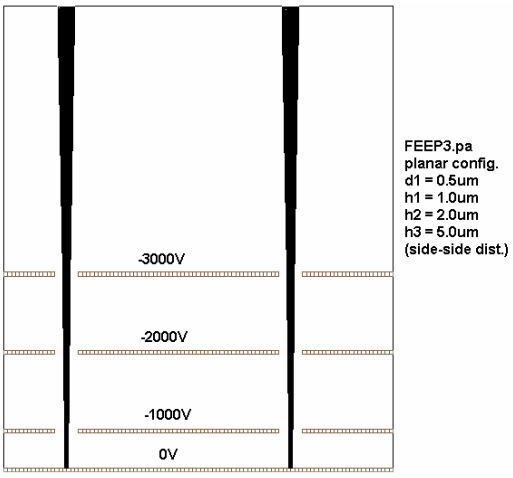

Figure 3: Two small vias shown extracting and accelerating either nano-particle or ions (likely separate vias for each kind).

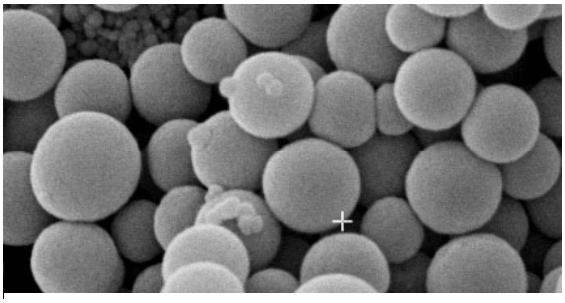

Figure 4: Example of a collection of unsorted nano-particles in the 100 nm diameter range[1].

As will be shown more quantitatively in a later section, the use of nano-particles in our nanoFET will allow for the ability to tune the I_{sp} and thrust over a very broad range at high efficiency. When little thrust with a high specific impulse is required, ions should be emitted. As thrust requirements go up, small nano-particles can be used to achieve slightly higher thrust and lower I_{sp}, and the larger nano-particles can be used for very high thrust and low I_{sp}. The range of thrust will be principally limited by the size, shape, and density of the particles, as well as the potential that they fall through.

The use of nano-particles should be contrasted with the formation of small droplets (colloid thruster). It is known that with the right emission current and temperature, charge extraction in FEEPs can produce instabilities that sometimes result in the formation of charged microscopic droplets (colloids)[5]. While these droplets could in principle be used to accomplish the same goal as our nano-particles, it is difficult to control their size and a distribution is expected. *Our nanoFET propulsion concept avoids the conditions that generate colloids and allows us to tune the nano-particle size independently of other factors.* Other benefits of our nanoFET approach include the use of multiple grids for high-finesse control of ion/nano-particle extraction and acceleration processes, robust material selection for field emission surfaces to ensure long life, and the use of separate ion and nano-particle emission zones to span the 100-10,000 s I_{sp} range. The multiple-grid design ensures that a large accelerating potential can be applied without exceeding the breakdown potential between adjacent grids. A two-dimensional ion trajectory simulation through multiple nanoFET grids (Figure 3) shows that ions/nano-particles experience steady acceleration through each grid and that the use of multiple grids helps to collimate the beam, thus minimizing spreading due to space-charge effects. Thus, by reducing beam divergence and by better coupling the grid potentials to the charged particles, our multi-grid approach improves the efficiency and likely lifetime of micron-scale field emission accelerators both at high I_{sp} with ions and at lower I_{sp} with charged nano-particles.

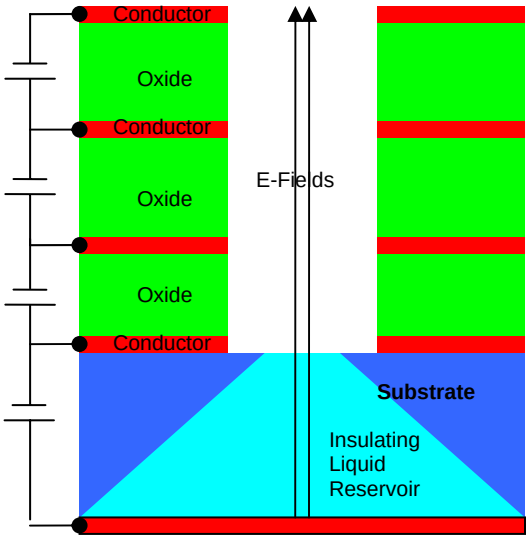

Figure 5: Structure of a single emitter, multi-grid nano-particle thruster using an insulating liquid

We envision the design of nanoFET as an extension to colloid thrusters, but emitting charged conducting nano-particles of known size and charge-to-mass ratios instead of charged liquid droplets which necessarily will have a distribution of sizes and charge-to-mass. Figure 5 depicts a model of a single emitter from the nano-particle thruster using an insulating liquid reservoir. These nano-spheres and cylinders would be fed into a liquid-filled reservoir and subjected to an electric field created by the acceleration grid. Particles that come into contact with the bottom electrode would become charged and pulled to the liquid surface by the electric field. If the electrostatic Coulomb force can cause nano-particles to break through the surface tension, field focusing should allow the particle to lift out of the liquid. Once extracted, the positively charged nano-particle would be accelerated by the electric field and ejected. It is also possible to consider with the same configuration a slightly conducting liquid where nano-particles arrive at the surface and are preferentially charged relative to the surrounding surface and therefore extracted in to the vacuum and ion optics region.

Note that neutralization of the charged particles is required. However, the concept of using MEMS-based technology to manufacture arrays of small vias with biased grids (just like nanoFET) to extract electrons is well known[5]. These are often called FEACs - Field Emission Array Cathodes. It is also possible to bias a separate section of the grid with opposite polarity and emit both positive and negatively charged particles, eliminating the need for a neutralizer when operating in the nano-particle mode.

II. The Physics Behind Nano-Particle Propulsion

A. Defining Thrust

Without getting into the details of extraction and acceleration of nano-particles, it is possible to understand how particle charge and mass both affect thruster performance. It is interesting to recast well-known propulsion equations to show the dependence on both the particle's mass and charge. First, thrust can be derived as

$$T = 2(q*n)*V_o*A, \tag{1}$$

where q is the charge of the nano-particle, n is the number density of particles, V_o is the potential difference applied across the accelerating grid(s), and A is the thruster area. The power is governed by

$$P = n*A*\left(\frac{2}{m}\right)^{\frac{1}{2}}(qV_o)^{\frac{3}{2}}, \tag{2}$$

where m is the mass of the particle. Now, dividing the thrust by the power, we obtain the specific thrust.

$$\frac{T}{P} = \left(\frac{2m}{qV_o}\right)^{\frac{1}{2}}. \tag{3}$$

The specific impulse is

$$I_{sp} = \frac{1}{g}\left(\frac{2qV_o}{m}\right)^{\frac{1}{2}}, \tag{4}$$

where *g* is the Earth's gravitational constant.

Note that the thrust-to-power ratio is *inversely proportional* to the square root of the charge-to-mass ratio of the particle while the I_{sp} is directly proportional to the same square root quantity. The importance of the charge-to-mass ratio lies at the foundation of some critical advantages of nano-particle propulsion over colloid thrusters and will be discussed in a later section.

B. Behavior of Nano-Particles in the Liquid Reservoir

Understanding the behavior of conducting particles in a liquid subjected to an electric field is of great importance to nano-particle propulsion technology. Most investigations of this topic have consisted of millimeter-sized spheres and cylinders placed in an insulating liquid between parallel planar electrodes with a potential difference applied between them[17]. Under the influence of an electric field, the particles become charged and bounce back and forth between the electrodes due to the Coulomb force, exchanging charge at every collision.

It is important to note that the following discussion only applies to the case when the liquid carrier is insulating. The easiest way to see how the particles are set into motion is to look at the forces acting on them, which are the Coulomb force and drag force:

$$F_c = qE \qquad (5) \qquad\qquad F_d = C_d\frac{\pi}{8}d^2\rho_l v^2. \qquad (6)^{16}$$

Here, q is the charge on the particle, v is the particle velocity, C_d is the coefficient of drag, and d is the particle diameter. Note that gravitational and buoyancy forces are neglected in zero gravity. To determine the equation governing the particle's motion, simply apply Newton's force equation to obtain

$$m\frac{d^2z}{dt^2} = F_c - F_d. \tag{7}$$

The particles' trajectories can be realized by numerically solving this equation.

It is possible to determine the charge acquired by a particle in contact with an electrode in the presence of an electric field by calculating the electric field intensity at the surface of the particle and applying Gauss's law. Felici predicted the charge acquired by spherical and cylindrical particles to go as[17]

$$q_{sph} = 4\pi r^2 \varepsilon_\ell \frac{\pi^2}{6} E \qquad (8) \qquad\qquad q_{cyl} = \frac{\pi \ell^2 \varepsilon_\ell E}{\ln\left(\frac{2\ell}{r}\right) - 1}, \qquad (9)$$

where r is the nano-particle radius, ℓ is the cylinder length, E is the electric field in the liquid, and ε_l is the dielectric constant of the liquid.

Once the particle begins to move away from one electrode, it will begin to lose charge to the liquid at a rate determined by the liquid conductivity (~$3.33*10^{-13}$ S/m for silicone oil). The charge loss will go as

$$q(t) = q_o e^{-t/\tau} \qquad (10)$$

where $\tau = \varepsilon_l/\sigma$ and is termed the electrical relaxation time constant. Therefore, in order to emit charged nano-particles, the electrical charge relaxation time should be large compared to the time it takes the nano-particles to be transported through the liquid to the surface.

Once the particles reach the liquid surface, the surface tension force will resist particle extraction. Surface tension is of great importance because it becomes a dominant force for particles at the micron scale and smaller. This is because it decreases linearly with the scale of the particle while all other forces decrease by a higher power. For example, the gravitational force is proportional to the volume of the particle and therefore decreases as a power of three. Similarly, the drag force is dependent on the surface area of a particle so it decreases as a power of two.

We are concerned with the ability to utilize an electric field to extract a charged nano-particle through the surface of a liquid. To approximate the minimum field strength and particle charge required for particle extraction, it is necessary to ensure that the Coulomb force is greater than the surface tension force, which is given as

$$F_s = \gamma \ell_{eff} \qquad (11)$$

where γ is the surface tension of the liquid and ℓ_{eff} is the effective radius of the particle. Setting the Coulomb force equal to the surface tension force and solving for the minimum required electric field for particle extraction, we obtain the following expressions for the spherical and cylindrical cases:

$$E_{sph,\min} = \sqrt{\frac{3\gamma \ell_{eff}}{2\pi^3 r^2 \varepsilon_\ell}} \qquad (12) \qquad\qquad E_{cyl,\min} = \sqrt{\frac{\gamma \ell_{eff}\left(\ln\left(\frac{2\ell}{r}\right) - 1\right)}{\pi \ell^2 \varepsilon_\ell}}. \qquad (13)$$

Returning to the thrust equations at the beginning of this section, we can see that the specific charge (charge-to-mass ratio) is very important in determining the thrusting performance. One advantage of nano-particle propulsion is the ability to control this parameter accurately as well as change it depending on the thrusting needs. The specific charge of spherical and cylindrical particles can be calculated to be

$$\left(\frac{q}{m}\right)_{sph} = \varepsilon_\ell \frac{\pi^2}{2r\rho} E \qquad (14) \qquad\qquad \left(\frac{q}{m}\right)_{cyl} = \varepsilon_\ell \frac{\ell}{\left(\ln\left(\frac{2\ell}{r}\right) - 1\right) r^2 \rho} E. \qquad (15)$$

Note that the specific charge of a spherical particle is dependent on the particle radius, density, and the applied electric field, and for the cylindrical particle the specific charge is dependent on the same variables with the addition of the particle length. This additional control parameter will allow for greater tunability. We will be considering both spherical and cylindrical particles as propellant sources. The cylindrical particles offer a greater specific charge range but may introduce other problems such as becoming entangled with others within the liquid reservoir (e.g. a carbon nanotube).

III. New Propulsion Levels of Performance Using Nano-Particles

Nano-particle propulsion provides important performance improvements over state-of-the-art ion, colloid, and possibly other thrusters in terms of thrust efficiency, specific impulse, specific thrust, thrust density, scalability, lifetime concerns, complexity of design, and specific mass.

A. Thrust Efficiency

Colloid thrusters are one approach to achieve similar claims as described here for nano-particles in a liquid carrier. However, nano-particles give greater control of specific charge of each particle. Further, the use of nano-particles should decrease the losses associated with Taylor cone formation.

A comparison of efficiency with other state of the art electrostatic thrusters is shown in Figure 6. The graph suggests that substantial improvements at both the low I_{sp} and high I_{sp} modes should be possible. Both nano-particle and ion emission modes of operation are shown.

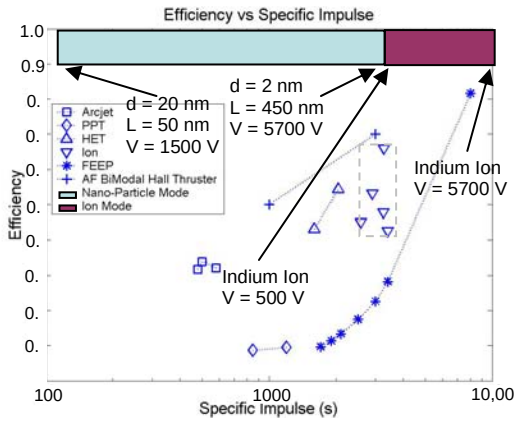

Figure 6: Improved efficiency for entire Isp range using nano-particles and ions[18]

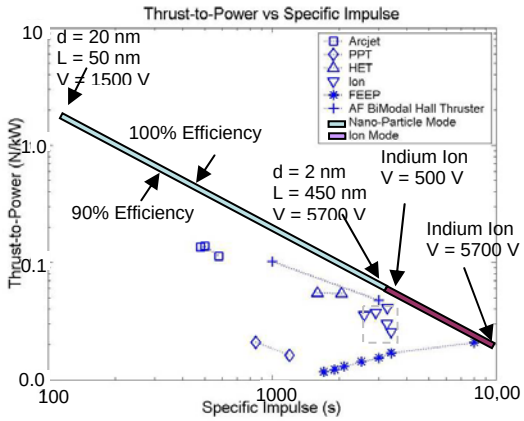

Figure 7: Highly scalable specific impulse and thrust-to-power using nano-particles and ions[18]

B. Specific Impulse and Specific Thrust Range

A significant improvement in the specific thrust and specific impulse range is possible if the specific charge of the particles can be adjusted and controlled. Figure 7 compares the expected specific thrust and I_{sp} when using cylindrical nano-particles with a length ranging from 20 nm to 270 nm, the radius ranging from 1 nm to 10 nm, and the accelerating potential ranging from 1500 to 9000 V to other state-of-the-art thrusters.

C. Thrust Density

State-of-the-art ion thrusters must operate substantially below the space-charge limit to assure proper ion-optic operation which would otherwise significantly increase sputtering damage and therefore decrease life-time. The ion thruster architecture is such that a slow moving ion plasma is drawn across a small gap. For nano-particles, we predict that a different analysis is needed. Isolated emitters operate independently of each other and the condition of importance is whether the amount of charge in the micron-sized hole is close to the charge determined by the capacitance across the gap (gate-to-propellant via). Further, even if nanoFET does approach an equivalent space-charge limit, since the charge may be contained in a fewer number of particles, it should be possible to operate much closer to this limit without degradation.

D. Thruster Lifetime

The lifetime of ion thrusters is limited due to erosion from charge exchange (CEX) collisions in the ion optics region and the discharge plasma source. The CEX collision occurs when a high energy ion collides with a low energy neutral and results in a low energy ion and a high energy neutral. The resulting ion strikes the conducting grid causing erosion. Both of these problems are eliminated when using nano-particle technology. Since only ions or charged nano-particles exist in the NEMS/MEMS grid structures there would be no charge exchange and because no plasma is generated, there would be no discharge plasma source.

E. Improved Specific Mass

While engine life is a critical constraint in many mission planning scenarios, a related and equally constraining thruster characteristic is specific mass. High thruster specific mass increases the mass of a space vehicle. This increase in vehicle mass can increase the needed "burn time" the thrusters must provide to accelerate the spacecraft to the required ΔV and places constraints on the spacecraft trajectory. For example, a heavy spacecraft would have to avoid certain orbits around moons in the Jovian system to minimize the risk of being captured or pulled in by the planetary body. Thus, increased system specific mass reduces the mission envelope the spacecraft can operate in.

Nano-particle technology addresses the specific mass through a number of design features. Ultra-long life could reduce the number of thrusters needed for a given mission. While individual conventional thrusters may be sufficiently light for a variety of missions, their insufficient lifespan means that multiple thrusters will be needed for a given "power slot" to accomplish the mission. For example, a 100 kW spacecraft will actually need eight 25-kW ion thrusters if the life of each engine is only half that required to fulfill the mission. In the example above, only four of the long-lived nano-particle thrusters would be needed. Moreover, the potentially higher thrust density of the thruster reduces the size of each thruster; i.e., one 100-kW thruster has less mass than four 25-kW conventional thrusters.

F. Simple Design

The "flat panel" concept (Figure 5) means that the propellant management system and power-processing unit are integrated right on the thruster, which reduces mass and integration complexity. Lastly, the "flat panel" thruster is smaller than conventional ion thrusters and will not need the magnets, grids, and discharge channel walls that account for the bulk of the mass of the latter.

IV. Conducting vs. Insulating Liquid Carrier

Further theoretical and experimental research will be required to determine which method of liquid carrier will work best: conducting or insulating. Both methods have their own advantages and disadvantages, which will be discussed in this section. The case of an insulating liquid carrier (Figure 5) was discussed in a previous section, where the particle is charged when it is in contact with the bottom electrode due to the presence of an electric field. Once the particle is charged, it would be transported to the liquid/vacuum interface by way of Coulomb's force. This force would continue to extract the particle through the liquid surface, accelerate, and finally eject it.

The case of a mildly conducting liquid would work much differently due to the absence of electric fields within the liquid (Figures 8). Since there are no significant fields in the liquid, another method must be devised to transport the particles to the liquid surface where they would be charged. Current ideas involve mixing the liquid (by heating, acoustic waves, etc.), which should allow particles to randomly approach the liquid surface. Upon approaching the surface, the (cylindrical) particles will align themselves, as suggested in Figure 9, due to polarization charging. If the electric field can focus on the tip of the particle, there will be preferential charging, and with sufficient charging the particle can be extracted through the

Figure 8: Single emitter of nano-particle thruster with conducting liquid.

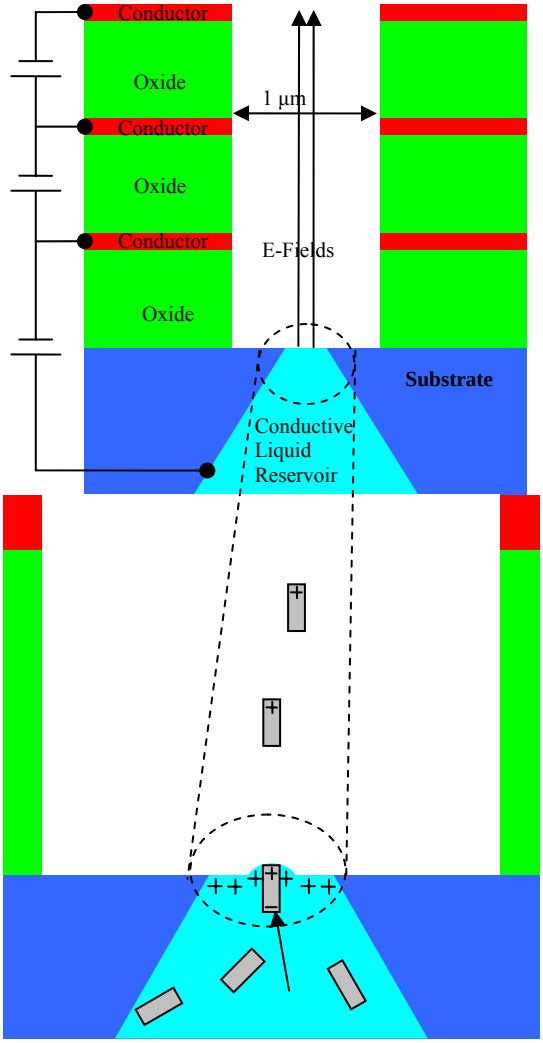

Figure 9: Nano-particles extracted and accelerated.

surface tension. An estimate of charge is given by equations 8 and 9 replacing ε_l with ε_o. Once charged and extracted, the particle would be accelerated and ejected just as in the insulating liquid case.

Since the behavior of the particles within the liquid is highly dependent on the conductivity of the liquid, there are several advantages and disadvantages of each scenario.

A. Advantages of an Insulating Liquid

- The transport of particles within the liquid to the surface can take advantage of electric fields that can be independently established.
- The movement of new particles into the reservoir may be handled in a similar manner by utilizing localized (pulsed) electric fields as well as other possible methods. This allows particles to be moved within the liquid, rather than moving the liquid itself.
- The formation of Taylor cones or other surface irregularities should be less likely and therefore particle emission should be more uniform.

B. Advantages of a Conducting Liquid

- The electric fields at the surface of the liquid should be normal to the surface and therefore more in the thrusting direction, which will help to prevent accelerating the particles into the grid structure.

C. Disadvantages of an Insulating Liquid

- The electric fields at the surface of the liquid may have components tangential to the surface, which may accelerate particles into the grid unless the particle is extracted near the center of the hole in the accelerating grids. This is because the particles reach a low terminal velocity within the viscous liquid and may not have the momentum to keep from being accelerated in the horizontal direction and into the grid structure.

D. Disadvantages of a Conducting Liquid

- The surface of the liquid would have charge density, which may induce Taylor cones of some sort.
- The movement of particles would require either moving the liquid along with the particles or some non-electric method (thermal, ultrasonic) to move just the particles.

V. Future Experiments

We are developing a series of initial experiments to better understand nano-particle propulsion. The objectives of these initial experiments are to 1) determine the behavior of particles in insulating and conducting liquids subjected to an electric field, 2) prove the feasibility of extracting particles from a liquid by way of electric field, and 3) identify appropriate liquid and nano-particle characteristics for in-space operation. Some experiments will be scaled-up, but we are also proceeding to develop micro-structure experiments.

Figure 10: First-generation MEMS gate design showing the viewing windows etched into the bulk silicon. Each viewing window contains tens of thousands of emission channels. The current MEMS gate is a second-generation design.

The micro-structure experiments will allow micro- and nano-sized particles and use a MEMS accelerating gate structure. MEMS gates are conducting grid structures that can be placed over a flat surface to apply an electric field to that surface. The advantage of the MEMS gate over metal screens is that they allow micron-scale or closer surface proximities, thus allowing the application of similarly strong electric fields as metal screens at modest voltages. These MEMS gates are currently being developed at the University of Michigan to be integrated with nano-structured surfaces such as cubic boron nitride and carbon nano-tubes for "tip-less" electron field-emission cathodes (FEC) and are being adopted for initial nanoFET experiments. Such FEC would be usable as a neutralizer for the nanoFET system to maintain charge balance during thruster

operation. A reversed bias on the MEMS gate could be used to provide the electric fields (~1E6 V/cm) needed to extract the nano-particles using modest bias voltages (< 300 V).

The MEMS gate consists of a conductive layer placed over a dielectric spacer with channels arrayed throughout the structure to permit passage of nano-particles or electrons. Use of micro-fabrication techniques enables the dielectric spacer to be made very thin, with the latest iteration of the MEMS gate having micron-scale dielectric thickness. By placing the conductive layer closer to the emission material; electric fields are concentrated and the bias voltage needed to achieve emission is reduced. Numerical simulations indicates that an approximate 1:1 ratio between the dielectric thickness and the channel diameter produces uniform field lines, so nano-particles used with the current iteration of the MEMS gate must have diameters on the order of hundreds of nanometers or less.

Gate layers are supported in a bulk silicon square with 1-cm sides. Ten viewing windows are etched in the bulk silicon to expose the emission channels, with each viewing window containing tens of thousands of emission channels. The top surface of the MEMS gate is a metal layer to facilitate wire bonds to the gate, and open regions are present that enable the gate to be clamped down upon the emission interface. Note that the present iteration of the MEMS gate is a prototype design that is undergoing optimization. More advanced micro-fabrication techniques will be employed in the future following device characterization and integrated testing. Optimizations include reducing the gap to decrease required extraction voltages and increasing the transparency. A stacked gate design is also under consideration to decouple the extraction and acceleration stages[14]. Figure 12 shows an older version of the MEMS gate design with 12 viewing windows instead of the current ten[15].

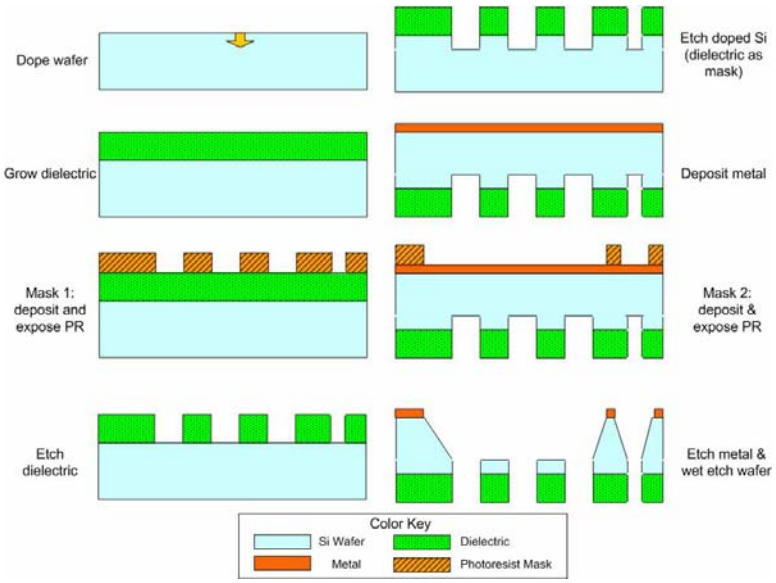

Figure 11: Gate fabrication process

The MEMS gates are fabricated via optical lithography and doped silicon wafers to minimize voltage drops within the gate. Micro-fabrication techniques used in the process are outlined below and are also shown in Figure 13.

1. One side of the silicon wafer is subjected to boron ion implantation to create a sub-micron thick region of highly doped silicon. This highly doped layer serves as the conductive gate layer and also as the etch stop for the final wet etch process. By using ion implantation rather than depositing a separate layer, a thin conductive layer can be formed to reduce gate current collection while still retaining sufficient structural robustness to resist rupture during gate handling and integration.
2. Low-stress silicon nitride of micron-scale thickness is grown on top of the highly doped silicon layer to serve as the dielectric spacer. The silicon nitride provides a slight tensile stress to keep the gate layers from peeling away from the bulk silicon. With a dielectric constant above 1E7 V/cm, silicon nitride is able to withstand the electric field strengths required for both nano-particle extraction and field emission.
3. Contact lithography is used to pattern the emission channels and backside scribe lanes. Spaced microns apart center-to-center, the emission channels are created using highly anisotropic reactive ion etch (RIE). The scribe lanes are also formed via RIE.
4. On the unprocessed side of the silicon wafer, a metal layer is deposited to form a surface that facilitates wire bonding to the MEMS gate. Good conductivity exists between the wire bond surface and the heavily doped gate layer due to the low resistivity of the bulk silicon.

5. Optical lithography is used to pattern the viewing windows and the front-side scribe lanes on the gold layer. A dissolved wafer process using ethylene diamine pyrocatechol (EDP) etches the viewing windows in the bulk silicon to expose the emission channels. With scribe lanes on both sides of the wafer, the gate structures are separated from each other as the final step of the EDP bath. This self-dicing prevents the particulate contamination and potential rupturing of the gate layers that could result from mechanical dicing.

To improve yield for the MEMS gates, test chips are included in the fabrication run to monitor each process step. These test chips would verify the presence of emission channels and the conductive ion-implanted layer following fabrication, and the test chips would also provide an indication of spatial variability during the fabrication process.

VI. Degrees of Freedom

The design of the nano-particle propulsion system leaves many degrees of freedom to obtain the ideal propulsion characteristics. There are three areas of the system that must be considered: the nano-particles, liquid in the reservoir, and the emitter.

The ability to choose the size, shape, and composition of the nano-particles gives rise to multiple options. As discussed before, we have the option to control the specific charge simply by determining the size and shape. This allows the thrust to power ratio to be varied easily. Other choices include the conductivity and density of the particles.

The choice of liquid will determine how the particles behave before and during extraction. Some important liquid characteristics are surface tension, viscosity, conductivity, polarity, permittivity, temperature effects, and behavior in a vacuum. For example, the surface tension will need to be strong enough to keep the liquid in the reservoir while weak enough to allow the particle to be extracted.

The size of the emitter opening and the gap between the grids offer more degrees of freedom. Note that the breakdown of the dielectric is around 300 V/μm[9].

VII. Conclusion

The investigation of the fundamentals of a MEMS/NEMS based flat-panel electric thruster along with the understanding of feasibility for nano-particle electric propulsion should provide important information on the prospects for an improved reliability and highly scalable propulsion system capable of operating over a large range of thrust and I_{sp}. Using MEMS/NEMS based field emission, it should be possible to improve lifetime by eliminating an ion thruster's discharge chamber and issues associated with CEX erosion in the ion optics region. Finally, it offers many degrees of freedom that allow it to be tweaked for the needs of various missions.

We are proceeding to investigate several fundamental questions about the nanoFET concept. Scaled experiments are being developed to validate the basic concepts for both emission and transport of the nano-particles.

VIII. Acknowledgments

Special thanks to Kimberly Appel and Robert Hower at the University of Michigan's Solid State Electronics Laboratory for their help in designing the MEMS gate fabrication process.

IX. References

1. Behan, Niall, "Nanomedicin and Drug delivery at the University of Limerick," The University of Limerick. http://www.ul.ie/elements/Issue4/behan.htm
2. Calero, J. "The electrohydrostatics of a Conductive Liquid Meniscus," IEEE 1988, p 1547-1551.
3. Chesta, E., Nicolini, D., Robertson, D. and Saccoccia, G., "Experimental Studies Related to Field Emission Thruster Operation: Emission Impact On Solar Cell Performances And Neutralization Electron Backstreming Phenomena," IEPC-2003-102, Proceedings of the International Electric Propulsion Conference, Toulouse, France, March 17-20, 20033 Choi, Changrag. "Dynamic Motion of a Conductive Particle in Viscouse Fluid Under DC Electric Field," IEEE Transactions on industry Applications, vol 37, No 3, May/June 2001.
4. Gallimore, A. "Micro Electric Propulsion Proposal," The University of Michigan, November 2003.
5. J.R. Brophy, J.E. Polk, V.K. Rawlin, Ion engine service life validation by analysis and testing, AIAA Paper 96-2715, JUly 1996.
6. Khayari, A. "The Charge Acquired by a Spherical Ball Bouncing on an Electrode: Comparison Between Theory and Experiment;" 2000 Conference on Electrical Insulatoin and Dielectric Phenomena.
7. Marcuccio, S. "Attitude and Orbit Control of Small Satellites and Constellations with FEEP Thrusters," Electric Rocket Propulsion Society, 1997.
8. Marcuccio, S. "FEEP Microthruster Technology Status and Potential Applications," International Astronautical Federation, 1997.
9. Marcuccio, S. "FEEP Thrusters," Nov. 1998, http://www.centrospazio.cpr.it/Centrospazio6FEEP.html.
10. M. Fehringer, F. Ruedenauer, W. Steiger, ESTEC Contract 12376/97/NL/PA Tech. Note No. 2, 1997.
11. Najafi, Khalil. Personal Communications, Univeristy of Michigan, 2004.
12. Stark, John. "Micro-Fabrication and Operation Nano Emitters Suitable for a Colloid Thruster Array," University of London, UK, https://escies.org/public/mnt4/S9.1Stark.pdf
13. Chock, R. "Photovoltaic & Space Environment Branch," NASA Glenn Research Center, July 2002, http://powerweb.grc.nasa.gov/pvsee/publications/tropix/Paper/AppA.html
14. Morris, D.P., Gilchrist, B.E., Gallimore, A.D., "Application of Dual Grids to Cold Cathode/ Field Effect Electron Emission, AIAA-2005-3669, 41st Joint Propulsion Conference, Tucson, AZ, July 10-13, 2005.
15. Goldberg, H., Encarnación, P., A., Morris, D., Gilchrist, B., Clarke, R., "Cold-Cathode Electron Field Emission of Boron Nitride Thin Film with a MEMS-Based Gate for Space Applications, AIAA-2004-3499, 40th Joint Propulsion Conference, Ft. Lauderdale, FL, July 11-14, 2004.
16. Tobazeon, R. "Behavior of Spherical and Cylindrical Particles in an Insulating Liquid Subjected to a DC Uniform Field." Laboratoire d'Electrostatique et de Materiaux Dielectriques. BP 166-38042 Grenoble Cedex 9 (France) pp. 415-420.
17. Felici, N. Rev. Gen. Elect., 75, pp. 1145-1160, 1966.
18. Wertz, Larson, "Space Mission Analysis and Design 3rd Ed." 1999